

## SPEED AND TENSILE FORCE CONTROL OF THE PULLING DEVICES OF THE CONTINUOUS LINE

by

**Saša S. NIKOLIĆ<sup>a\*</sup>, Igor B. KOCIĆ<sup>a</sup>, Dragan S. ANTIĆ<sup>a</sup>, Darko B. MITIĆ<sup>a</sup>,  
Nikola B. DANKOVIĆ<sup>a</sup>, Miroslav B. MILOVANOVIĆ<sup>a</sup>, and Petar S. DJEKIĆ<sup>b</sup>**

<sup>a</sup> Faculty of Electronic Engineering, University of Niš, Niš, Serbia

<sup>b</sup> The Academy of Applied Technical and Preschool Studies, Niš, Serbia

Original scientific paper

<https://doi.org/10.2298/TSCI230418138N>

*In cable production, it is imperative to control speed and tension. This paper proposes a web tensile force regulation between input and output pulling caterpillar devices. The web tensile force is controlled indirectly using a PI controller based on feedback information about tensile force using a tensile observer. This paper also deals with the regulation speed of the input-pulling caterpillar device and the speed and torque (current) of output pulling caterpillar device and deals with the effect of line speed on the temperature change at the extruder zones. The input and output-pulling caterpillar devices are connected by the web material that is processed on them. The input and output-pulling caterpillar devices are connected by the web material that is processed on them. The task was realized using a programmable logic controller Micrologix 1200 controller and SIMOREG DC drives, which regulate the input caterpillar's speed and output caterpillar's torque. The identification of separately excited DC motors parameters was made. Models for the input, output caterpillars and web zone were simulated in MATLAB and SIMULINK. The controllers of the current loop, velocity loop, and tension loop are all integral isolated PI regulators. Speed signal is obtained by tachogenerator. In practical realization, tensile force is observed directly from the Simoreg DC converter, eliminating the tension sensor. The tensile force controller is realized with the PI controller, which was realized with programmable logic controller. Setting optimal parameters is performed using ITAE criteria. The ITAE function is calculated using a complex Simpson's quadrature formula.*

*Key words: programmable logic controller, pulling caterpillar device, Simoreg DC master controller, torque, PI controller, tensile controller*

### Introduction

A tensile force control system for proper tensile control is applied in industries to produce paper, cable, fiber, etc. [1]. In the cable production industry, improper tension control will damage and stretch the conductors and cables. The tension control system is a highly non-linear multivariable system. The problem that needs to be solved is controlling each line drive speed while maintaining a constant tension force within the given limits. There are two ways to regulate the tension: direct control (with a tension sensor) and indirect control

\* Corresponding author, e-mail: sasa.s.nikolic@elfak.ni.ac.rs

(without a tension sensor) [2, 3]. In the process section, the conductor is placed between the tracks. Speed and tension control systems also depend on process uncertainties, such as slippage between the conductors of the tensioning force transmission device and the applied rollers, irregularity of the shape of the rollers due to wear during operation, *etc.* because that, choosing the right type of controller for the system and controller setup is not simple. Direct regulation methods are almost always used, which require the measurement of the current tensile force. An additional sensor for measuring the amount of tensile force requires adding a roll system, which, together with the tension sensor, further increases the cost of regulation. Therefore for low cost, it is necessary to make a tension observer. The paper presents a tensile control method where the current value of the speed, current and tension is obtained directly from the outputs of the Simoreg DC controllers. Also, the current value of the armature current of the output-pulling caterpillar device can be easily obtained through the observer of the armature current of the output-pulling caterpillar device. This paper describes the method, software and hardware for regulating the speed and tension force of input and output caterpillar, which achieves constant tensioning of the conductor on. The tensile force of the DC motor is proportional to the armature current.

The programmable logic controller (PLC) is an essential part of any industrial control system. Actual tensile force proportional to the motor's torque was transferred to the analogue input of PLC using the analogue output from the DC controller. Desired torque (tensile force of the conductor) is set using a potentiometer or HMI panel. Actual motor speed transferred to PLC using by shaft tacho generator and converted card. According to the input signal and software, the PLC controller generates an analogue signal for torque (tensile force) control. By setting the torque of the DC motor, the tensile force of the conductor is set by using DC motor and output pulling caterpillar device which it drives. Using the PID command of the PLC controller, the PI regulator for the DC motor current was realized. In contrast, the cascade control loop in the motor controller was broken so that the PLC controller PI regulator performs the motor armature current regulation. The DC motor speed is limited to the rated speed. The DC motor model, DC regulator was identified, and the characteristics of armature voltage, armature current and motor speed were recorded. The moment of inertia of the motor at idle was determined. After that, a simulation was done in MATLAB and SIMULINK. The results were experimentally verified on the input and output caterpillar devices of the Johne Royle and Bartell Company. The method of technical optimum was applied for the synthesis of the regulator.

### **Mathematical model of pulling caterpillar**

A schematic diagram of a continuous extrusion line with two pulling caterpillar devices is shown in fig. 1 [3-5]. For more effortless synchronization, both pulling caterpillar devices have an identical construction and drive motors with the same characteristic. The continuous extrusion line consists of several parts, an unwinder, a processing section and a winder. The unwinder device No. 1 is used for unwinding, and the winder device is used for winding finished product No. 6. The processing section consists of the following:

- the input-pulling caterpillar device serves to pull the cable from the unwinder device. It is the leading device of the line, and it works in speed mode. All devices are synchronized to their speed No. 2,
- the extruder (extruders) serves to apply a layer of insulation over the conductor cable No. 3,
- the cooling trough has the role of cooling the conductor before it enters the output-pulling caterpillar device in order to prevent its deformation No. 4, and

- the output-pulling caterpillar device serves to tow the product with a constant torque. It works in the torque mode and should maintain a constant tension force of conductor No. 5.

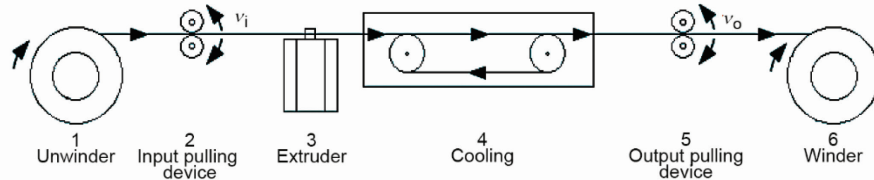


**Figure 1. Block diagram of a continuous extrusion line with two caterpillar cable pulling devices**

In the processing section conductor is placed between the caterpillars, passes through the extruder head, and is cooled by passing through the cooling trough. When caterpillars are closed, the motor torque is transmitted *via* the gearbox onto the pulleys and then to the caterpillars. Each caterpillar device consists of the following parts: motor, belt, gearbox, caterpillar, and opening and closing system.

The following assumptions were made during analyze and development of mathematical modeling:

- traction devices are shaped like ideal rollers,
- the entire transmission system from the motor to the conductor is observed through the transmission ratio of the reducer action devices are shaped like ideal rollers,
- occurrences of slipping between the net and the support rollers are not considered,
- the friction model is linear,
- working conditions are constant,
- it is assumed that the web is a material (conductor) with a large Young's modulus of elasticity and that it is a viscous elastic material, and
- input and output pulling caterpillar has identical electrical and mechanical characteristics.

The following equations can describe the behavior of the system in figs. 2(a) and 2(b) [6-10].

$$\frac{d}{dt}(J_i \omega_i) = M_i + M - M_{ir} - B_i \omega_i - M_{ai} \quad (1)$$

$$\frac{d}{dt}(J_o \omega_o) = M_o - M - M_{or} - B_o \omega_o - M_{ao} \quad (2)$$

$$F = \frac{ES}{L}(v_o - v_i) + \frac{CS}{L} \frac{d}{dt}(v_o - v_i) \quad (3)$$

$$k_s = \frac{ES}{L}, \quad d_s = \frac{CS}{L} \quad (4)$$

Equations (1) and (2) describe the dynamic behavior of the input and output caterpillars: where  $J_i$  and  $J_o$  are the moments of inertia,  $B_i$  and  $B_o$  are viscous friction coefficients,  $M_{ir}$  and  $M_{or}$  are coulomb friction,  $M_{ai}$  and  $M_{ao}$  acceleration-deceleration torque of the input and output pulling caterpillar device reduced to the shaft of the drive motors respectively,  $M_i$  and  $M_o$  are motor torque of the input and output pulling caterpillar device, and  $M$  is a torque which is corresponding to the tensile force  $F$ . Equation (3) describes the viscous elastic model (Vought model) of material is placed between the caterpillars,  $F$  is the tensile force,  $E$  is the modulus of elasticity,  $C$  is the web material dampening coefficient,  $S$

cross-sectional area of material, and  $L$  is the distance between caterpillar. Spring constant  $k_s$  and constant damper  $d_s$  are given in eq. (4). Based on these equations, it can be seen that the variation of any of the listed parameters affects the amount of tension.

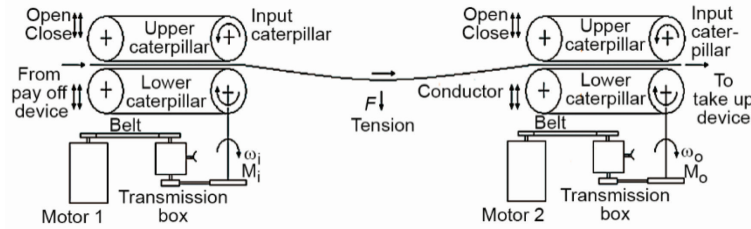


Figure 2(a). Block diagram of tension zone between input and output pulling caterpillar devices

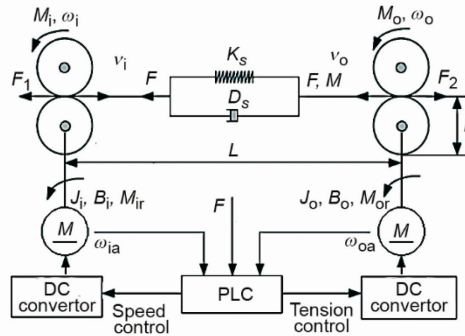


Figure 2(b). Block diagram of tension zone between input and output pulling caterpillar devices

Table 1 shows the parameters of the web for round copper wire.

Table 1. Web parameters

Parameters	Values
Spring constant, $k_s$ , for $C_u$	$3.65 \times 10^3$ N/m
Damper constant, $d_s$ , for $C_u$	$\approx 0$ Ns/m
Distance, $L$	60 m
Cross area, $S$	$2.5 \text{ mm}^2$
Viscous damping ratio, $\zeta$	$< 0.001$

In eq. (5)  $M_{ti}$  and  $M_{to}$  are the torque required to maintain a given tensile force  $F_r$ , which are equivalent to the moment  $M$ , the  $r$  is the diameter of the roll, and the  $i_n$  is the total gear transmission ratio of reduction. The acceleration moment is given by eq. (6), it occurs when accelerating and decelerating the line. In eq. (7), the total moment of inertia  $J$  reduced to the drive motor shaft is given. It consists of the moment of inertia of the  $J_m$  drive motor,  $J_s$  the moment of inertia of the shaft and  $J_d$  is the moment of inertia of the caterpillar pulling device:

$$M_{to} = M_{ti} = M = \frac{F_r r}{2i_n} \tag{5}$$

$$M_{ai} = J \frac{d\omega_i}{dt} = J \frac{2i_n}{D} \frac{dv_i}{dt} \quad (6)$$

$$J = J_m + \frac{J_s + J_d}{i_n^2} \quad (7)$$

Due to the requirement to change insulation material or the color of the conductor insulation, the line speed changes along a ramp from zero to the set value as shown in the figure, where the parameter  $t_u$  represents the acceleration time and  $t_d$  the deceleration time, fig. 3.

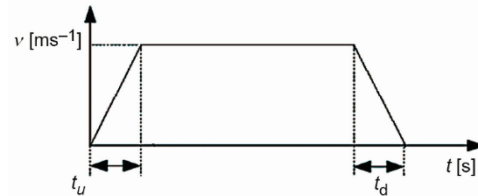


Figure 3. Ramp function

In order to maintain a constant tensile force, it is necessary to measure or somehow determine the current value of tensile force. For this purpose, it is necessary to design the tension observer, and determine the transfer functions of the motor armature part, the mechanical part of the DC motor, the DC regulator, the armature current measuring element and the pre-filter of the current measuring element. If we ignore the Coulomb

friction, we can consider that the moment  $M$  corresponding to the actual tensile force is proportional to the moment  $M_o$  and viscous friction. The motor torque directly depends on the armature current. Current speed and armature current are easily obtained from the output of the applied regulator. These values are scaled using the PLC controller to match current and speed values. The torque responsible for the desired tension can also be calculated from the tension set point, the gear transmission, and Coulomb friction.

The tension observer [8, 11, 12] can be implemented based on drive torque related to the tension zone. Tensile force  $F$  corresponding to the torque  $M$  can be determined by analyzing the torque eqs. (1) and (2). Torque  $M$  can be considered constant during the sampling frequency time, and Coulomb friction  $M_{or}$  can be obtained by experiment in the offline state. We consider the moment of inertia of output-pulling caterpillar  $J_o$  to be constant, so one (2) is approximated:

$$\begin{aligned} \frac{d}{dt}(J_o \omega_o) &\approx J_o \frac{d\omega_o}{dt} = M_o - M - M_{or} - B_o \omega_o \\ \frac{d}{dt}(M) &= 0 \end{aligned} \quad (8)$$

Equation (8) can be written in the form of a state space model:

$$\begin{aligned} \begin{bmatrix} \dot{\omega}_o \\ \dot{M} \end{bmatrix} &= \begin{bmatrix} -\frac{B_o}{J_o} & -\frac{1}{J_o} \\ 0 & 0 \end{bmatrix} \begin{bmatrix} \omega_o \\ M \end{bmatrix} + \begin{bmatrix} \frac{1}{J_o} \\ 0 \end{bmatrix} (M_o - M_{or}) \\ \begin{bmatrix} \omega_o \end{bmatrix} &= \begin{bmatrix} 1 & 0 \end{bmatrix} \begin{bmatrix} \omega_o \\ M \end{bmatrix} \\ \dot{x} &= A\bar{x} + Bu, \quad y = C\bar{x} \end{aligned} \quad (9)$$

The observability matrix of state space model (9) has  $rank = 2$  which is a necessary and sufficient condition for the synthesis of the tension observer. For model (9) the tension observer is given by [8]:

$$\begin{aligned}\hat{\dot{x}} &= A\hat{x} + Bu + \bar{k}(y - \hat{y}) \\ \hat{y} &= C\hat{x}\end{aligned}\quad (10)$$

where  $\hat{x} = [\hat{\omega}_0 \quad \hat{M}]^T$ ,  $y = [\omega_0]$ , and  $\bar{k} = [k_1 \quad k_2]^T$ . For the tension observer to be stable, it is necessary to choose a  $k$  so that the roots of the characteristic equation are with negative real parts. In the input and output pulling caterpillar device system, the moments of inertia of both devices can be considered constant.

**Table 2. Motors parameters**

Parameters	Values
Motor power, $P$	15 HP
Armature voltage, $U_a$	400 V
Armature current, $I_a$	27.2 A
Motor speed, $n$	1550/2300 rpm
Excitation voltage, $U_p$	300/150 V
Excitation current, $I_p$	1.6/0.88 A
Armature winding resistance, $R_a$	1.51 $\Omega$
Inductance of armature winding, $L_a$	34.68 mH
Excitation winding resistance, $R_p$	132.7 $\Omega$
Electromotive force constant, $k_e$	2.442 V
Viscous friction coefficients, $B$	0.00712 Nms
Moment of inertia, $J$	0.0163 kgm <sup>2</sup>

Transfer function and simulation model for DC converter [13-19], model and parameters of armature current controller for output caterpillar pulling device, model and parameters of velocity controller for input caterpillar pulling device taken from [12], tab. 2.

### Analysis of the effect of line speed on temperature transfer through the extruder

In identifying and determining the process model of extruder [20], we started from the FOPDT model (10), which approximated the process. Experimental results were obtained on Royle 4\_1/2" extruder for PVC insulation. The parameters of the model are determined based on the step response of the open loop and Streitz method [21, 22]. To determine the parameters  $T_u$  and  $T_{ob}$ , a program was written in MATLAB.

$$G_{ob}(s) = \frac{k_{ob}}{1 + sT_{ob}} e^{-sT_u} \quad (11)$$

Based on the measurements, it is clear that the times  $T_u$  and  $T_{ob}$  for zone 2 are higher when only zone 2 is heated. It can also be seen that when zones 1, 2, 3 are heated, that zone 2 reaches the temperature the fastest. If the analysis of the ratio  $T_{ob}/T_u$  is performed, it is concluded that it is impossible to determine the characteristics of the process described by the  $PT_2$  model according to Streitz's identification method [22]. After that, models were determined for all three zones based on the  $PT_n$  model (11) [22], where  $T$  is the process time constant,  $n$  is the order of the  $PT_n$  model,  $T_{ob}$  is the object gain taken from the FOPDT model. A 3-order model was determined. Table 3 gives the values first only for zone 2 when only it is heated, and then for zones 1, 2, and 3 that are heated at the same time.

$$G_{ob}(s) = \frac{k_{ob}}{(1 + sT)^n} \quad (12)$$

**Table 3. Time constant of  $PT_n$  model,  $n = 3$**

	Only zone 2 is heated	Zones 1, 2, and 3 are heated at the same time		
	Zone 2	Zone 1	Zone 2	Zone 3
$T$ [minutes]	5.710	4.507	4.3887	4.643

In general, eq. (12) applies equation to the simulation model where ( $i = 1, \dots, n - 1$ ) is denoted by observed zone of the impact of zones  $i - 1, i, i + 1$ .

$$T_{zi}(s) = G_{obzi}[u_i + k_{z(i-1),i}T_{z(i-1)} + k_{z(i+1),i}T_{z(i+1)}] \quad (13)$$

When simulating the mutual influence of zone heating, all zones are identified separately. This means that it is necessary to heat only the observed zones, make its model, and cool it and its neighboring zones. Repeat the procedure for all zones observed. In this way, the coefficient  $K_{z22}$  can be determined by comparing the influences when the heated zones are individually and all at once, so model (12) is applied for the simulation. Heat transfer coefficients were observed when the extruder is in the process of heating, the same applies to cooling. Figure 4 shows the model of the mutual influence of the zones.

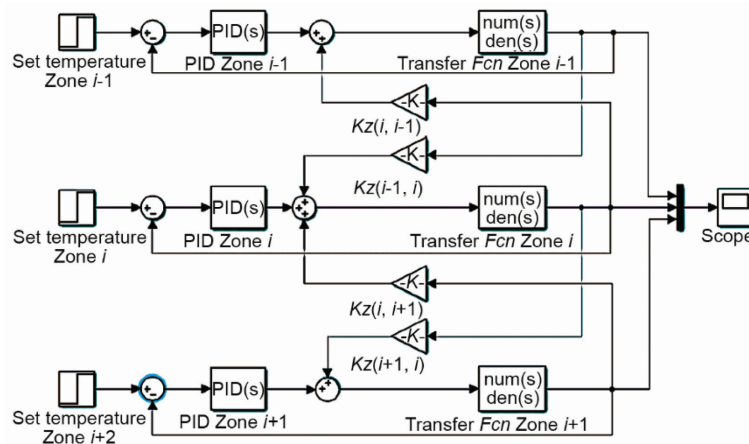


**Figure 4. Model of mutual influence of zones**

All of these considerations apply to a line at rest. When the line starts, the speed of the extruder screw changes according to the speed of the line. In this regard, the influence coefficient of the previous zone on the next zone in the simulation should be increased by a certain percentage, and the influence coefficient of the next zone on the previous one should be decreased by a certain percentage.

Figure 5 shows response of temperature when the influence simulation analyze using simulation model in MATLAB from fig. 4. The PID parameters for heating zones are taken from [20]. Temperature response for a set desire zone temperature of 200 °C, and the mutual influence of 1, 2, and 3 zones taken with the coefficient  $k_{z12} = k_{z21} = k_{z23} = k_{z32} = k = 0.1$  fig. 5(a), and  $k_{z12} = 0.15$ ,  $k_{z21} = k_{z23} = 0.1$ , and  $k_{z32} = 0.8$ , fig. 5(b).

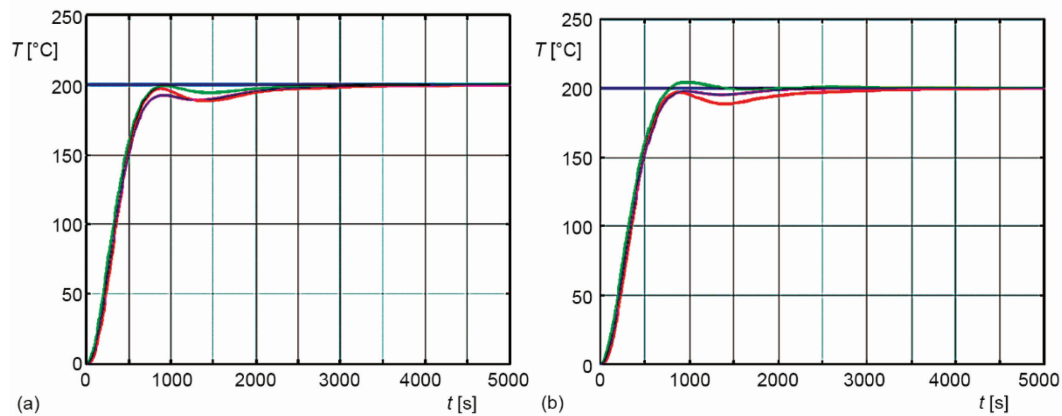


**Figure 5. Model of mutual influence of 1, 2, and 3 zone, set temperature (blue), temperature zone 1 (red), zone 2 (green), and zone 3 (magenta)**

The mutual influence of the zones changes with the change of line speed, as the coefficient of, as the coefficient of influence of zone  $i$  on zone  $i + 1$  increases, and the coefficient of influence of zone  $i - 1$  on zone  $i$  decreases, which is logical because the temperature gradient in the extruder cylinder is directed in the direction of mass movement through it. The mutual influence of zones during the simultaneous heating or cooling of the extruder when the line is in stop mode can be simulated by a constant coefficient of mutual influence.

### Synthesis of the tensile force controller

The PI tensile force controller parameters are set using ITAE criteria [23]. The optimal values of the PI controller are determined [12, 24], which minimizes the goal function (15). The integral of the eq. (13) is calculated using a complex Simpson's quadrature formula that is based on interpolation (16) [21, 23, 25], and in accordance with it, the program is written in MATLAB. The program in MATLAB as variables uses the controller parameters:

$$e(t) = F_r - F(t) \quad (14)$$

$$J = \int_0^{\infty} t |e(t)| dt \quad (15)$$



$$\int_a^b f(x)dx \approx \frac{h}{3} \left( f_0 + 4 \sum_{i=1}^m f_{2i-1} + 2 \sum_{i=1}^{m-1} f_{2i} + f_{2m} \right) \quad (16)$$

$$h = \frac{b-a}{m}, \quad f_0 = f(a), \quad f_{2m} = f(b) \quad (17)$$

In eqs. (16) and (17)  $a$  and  $b$  are the endpoints of integrations, the interval of integration  $[a, b]$  split up into  $m$  sub-intervals,  $m$  is an even number,  $h = (b - a)/m$  is the step length,  $m$  is the midpoint of integration interval  $[a, b]$ . The linear PI controller of the input-pulling caterpillar devices is adjusted using MATLAB and SIMULINK.

The setting procedure consists of the following steps.

- For a closed loop feedback system with the known transmission function, the critical gain  $(k)_{kr}$  and cross phase frequency  $(\omega_\pi)_{kr}$  are determined by using a suitable written program in MATLAB.
- For the initial values of the regulator parameters, the values for  $k_p$ , and  $k_i$ , are determined by the Ziegler-Nichols rule for a closed-loop system.
- The values of parameters from the points  $k_p$ , and  $k_i$  are used as the initial values for solving the integral (16) and (17).
- In SIMULINK, the model of the process with the appropriate regulator is drawn.
- Using the suitably written MATLAB script for the integral solution eq. (15), the toolbox optimization and SIMULINK system model, the optimal parameter values of the controller  $k_p$ , and  $k_i$  are determined by the criterion (16).

### Synthesis of control strategy for input and output caterpillar pulling device

The pulling caterpillar device drive model consists of a PI speed controller, PI current controller, DC converter model, motor model and mechanical part.

The optimal technical method calculates the PI current controller, and the PI speed controller is determined by setting the poles for the desired closed-loop transfer function. Both controllers have blocks for limiting the maximum and minimum current (torque) and maximum and minimum speed. The input and output device system model in fig. 6 consists of the ramp generator model, the input and output pulling caterpillar model, the web model of the conductor that is processed on them, and the PI tensile force controller.

The model of the ramp block generates a function to change the speed according to the ramp, see fig. 3. It simulates the starting and stopping of the line based on the set speed and the magnitude of the change in acceleration and deceleration of the line. It can be used to observe the moment of acceleration and deceleration and their compensation. The input-pulling caterpillar device is the primary device on the line. It is the master of the line, while all other devices and the output-pulling caterpillar device (slave) follow his speed. Output-pulling caterpillar device has a preset torque limit. A PI tensile force controller generates the desired tensile force for the line in the run or stop mode, fig. 7.

Figure 8(a) shows the input traction device speed responses for a given input-pulling caterpillar device speed of 140 rpm, corresponding to a line speed of 18 m/s. Figure 8(b) shows the torque response of the input and output pulling caterpillar device for a given tension force of 15.6 Nm, which corresponds to a current difference of 4 A.

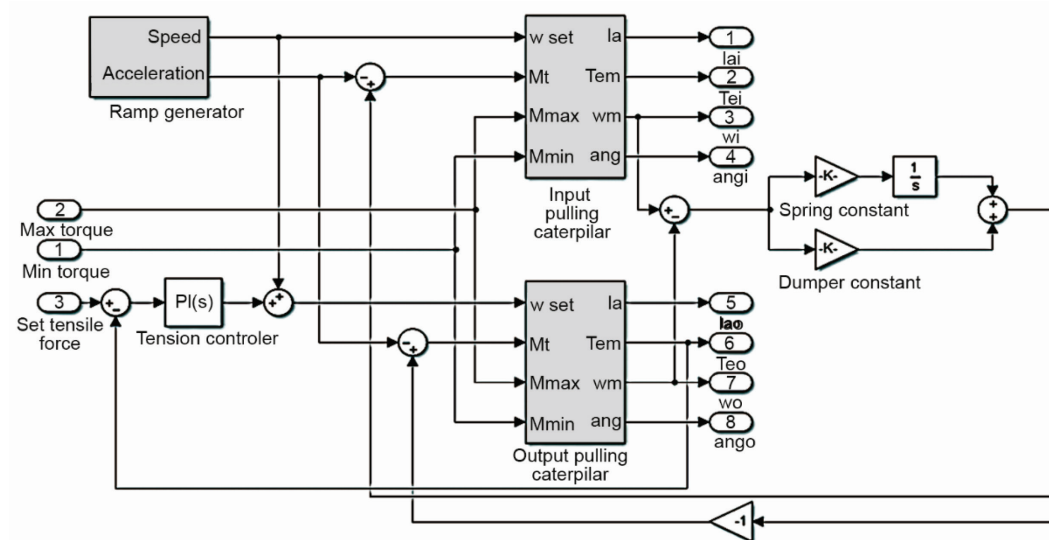


Figure 6. Block diagram of tensile force control

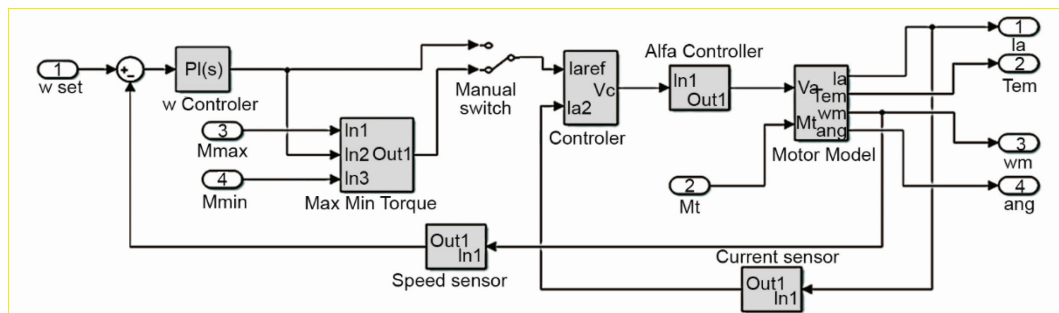


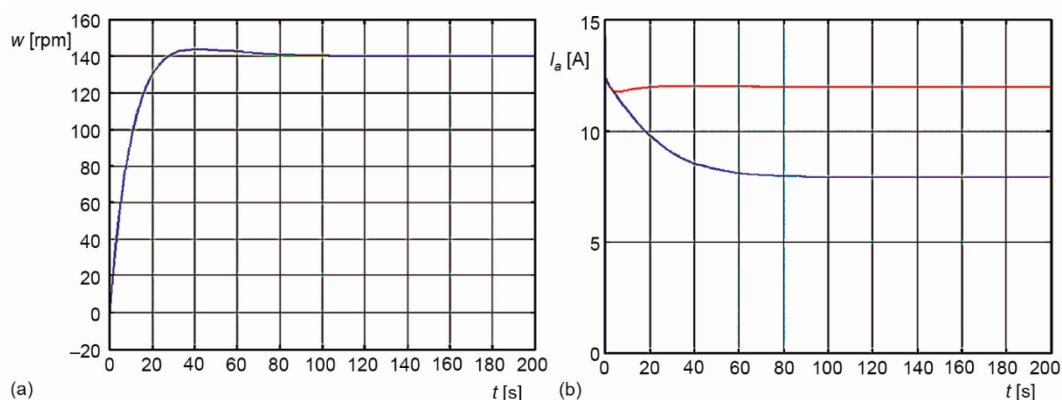
Figure 7. Block diagram of model pulling caterpillar device with velocity and torque controller

Figure 9(a) shows the difference in angular velocities of the input and output pulling caterpillar device. Figure 9(b) shows the torque difference between the output and input-pulling caterpillar devices represented over their armature current.

### Experimental results

The tensile force control was experimentally tested on a Bartell input and output pulling caterpillar device driven by a Reliance DC motor with the characteristics already mentioned and represented over the block model, see fig. 10. The PLC software was written in LAD language using Allen Bradley's RSLOGIX V8.2 software, the panel software was written in an Internet Browser. The Simoreg DC Master controller uses Siemens DRIVEMONITOR software [12, 23].

The control task was realized using a PLC controller Allen Bradley Micrologix 1200, with a module for Ethernet communication 1762 NET ENI [26] and DC controller Siemens Simoreg DC Master 6RA7030 6DV62 [6], which can work in four quadrants. Line operation is monitored *via* the HMI PanelView C1000.



**Figure 8.** Speed response in time of input pulling caterpillar device (a), and tensile force response of input and output pulling caterpillar represent over armature current (b), red is output, blue is of input pulling caterpillar device

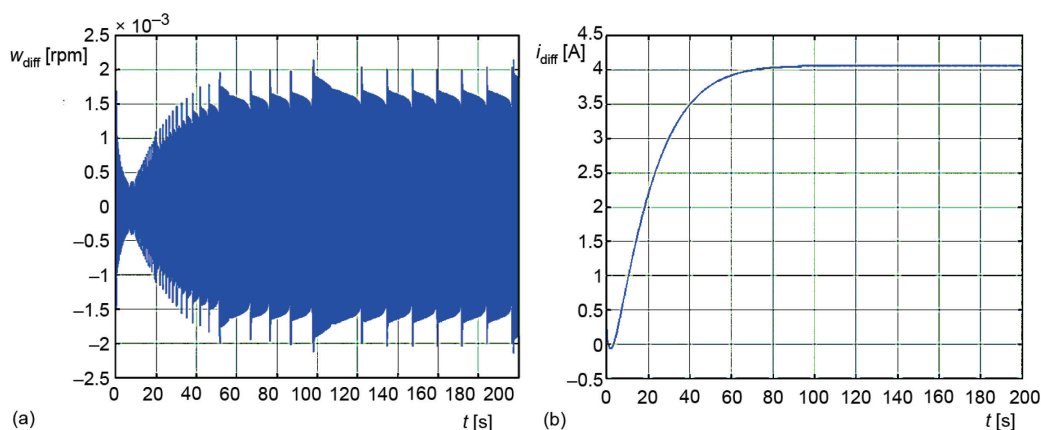


**Figure 9.** Difference speed of input and output pulling caterpillar device (a), difference of torque of input and output pulling caterpillar device represent over difference of armature current (b)

A tachogenerator is connected to the input of the CUD1 XT 103,104 [6], which gives 87.5 V at 1000 rpm. The motor speed value given by Simoreg is connected to an analogue input of PLC. By entering the parameters  $P83 = 1$  and  $P741 = 135.625V$ , a tachogenerator was chosen to measure the current rotor speed to limit the maximum rotation speed with parameters  $P512$  and  $P513$  [6]. The armature current that also defines the desired tensile force is set by the potentiometer and led to the analogue input of the PLC controller module, scaled and processed, and used as the set point of the PI current controller PLC. The currents values of the armature current of both motors are measured using a Simoreg controller and from its output CUD X175 12.13, which leads to the input of the analogue module of the PLC controller where it is scaled and processed, as such used as the current value for the PI controller current of the PLC controller. The value of the control voltage of the PI current regulator from the output of the analogue module is fed to the input CUD1 X 174 4, 5. By a suitable connection of the function diagrams of the Simoreg controller, the control signal is connected to the input of the controller function diagram G113. Connector

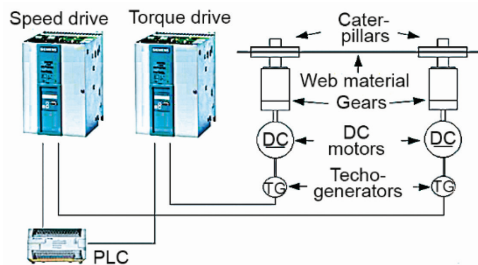


**Figure 10. Drives and components of experimental test**

and displayed together with the set current (torque) value on the HMI panel. This provides immediate insight into the quality of regulation. Analogue modules are set to a signal value of 0-10 V. The PI armature current regulator was realized using PID instruction [27-31].

The step excitation is realized by setting the desired armature current with the potentiometer, and then the output caterpillar device is started, which also starts the PI tensile force controller. The time scale is given in the scale of 0.1 seconds because the set period for data acquisition is set to 100 ms. In fig. 11, the response to when a given current is randomly increased in the range of 0 A to 2.8 A is shown. Figure 12 shows the response characteristic, with a jump change of the given tensile force over a current of 1 A in time intervals of 2 seconds each. A response was obtained for current reinforcement values of 2 A, 3 A, 4 A, and 5 A. Figures 13 and 14 shows the characteristic of the motor armature current of the output-pulling caterpillar device corresponding to the tensile force when the line speed changed from 18 m per minute to 20 m per minute. The tension is constant with the change in speed.

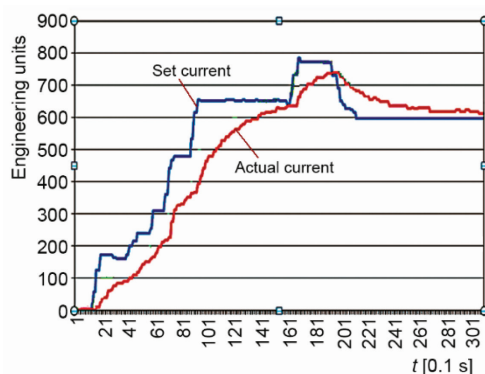


**Figure 11. Response to a change in the set current from 0 A to 2.8 A, current is randomly increased**

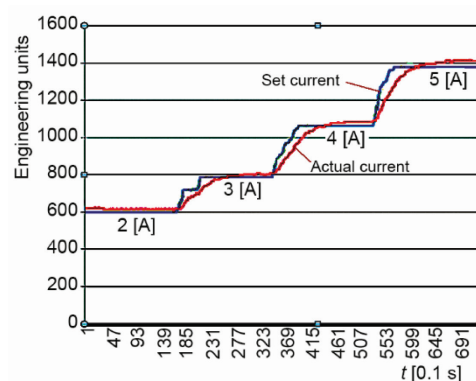


**Figure 12. Response with a jump change of the given tensile force over current of 1 A in time intervals of 2 seconds each jump**

## Conclusions

This paper proposes a novel tensile force controller method based on ITAE criteria that do not need additional hardware for measured current tension. Current tension is obtained from the output of the Simoreg DC master controller. Input pulling caterpillar motor adjusts

K0015 is connected to parameter P500 from the function diagrams G160. Parameter P084 = 2, function diagram G160, breaks the cascade control loop of speed and current. The role of the PI controller of the DC controller [25] is taken over by the PI controller realized by the PLC controller.

The actual current (torque) value is taken from the analogue output of the Simoreg DC controller for both pulling caterpillar device read and entered in registers I:2.1, I:3.1 of the PLC controller, scaled with the SCP command

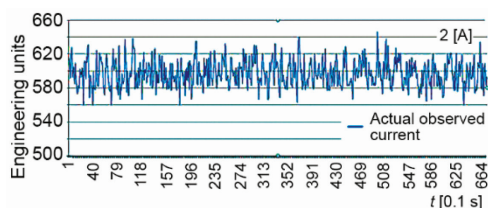


**Figure 13. The characteristic of the motor armature current of the output pulling caterpillar device corresponding to the tensile force when the line change from 18 m per minute to 20 m per minute**

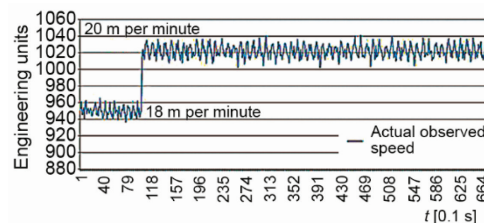


**Figure 14. The characteristic change the line speed from 18 to 20 m per minute**

the linear velocity, and the output-pulling caterpillar motor controls the tension. Controlling the tensile force was achieved by using the speed controller of the input-pulling device as the master speed and tension as the slave. Slave drive has a preset torque limit. The master drives maintain the line speed to the desired value. It is vital to compensate for the moment of inertia during running.

For this reason, the compensation signal is added to the required tensile force. The signal for linear velocity and tension is given from the PLC controller. Simoreg DC Master regulators using satisfactory results were obtained by the torque (tension) control procedure. Using an external PI tension (armature current) regulator realized by exploiting a PLC controller significantly improved the regulation of the output caterpillar motor armature current (torque). When speed is not controlled and limited, the only disadvantage of this type of regulation is reflected when starting the engine that is not loaded. Its speed increases to a speed limited by the mechanical load of the engine and load. The speed can be limited by setting the controller parameters to maximum and minimum speed, introducing a maximum speed signal from the input caterpillar device, or using the PI speed controller method. The presented method has shown practical value in industrial applications for producing conductors and cables. The derived model of the mutual influence of the extruder zone in the operation of the line can serve well for the analysis of the influence of line speeds on heat transfer in the extruder.

## References

- [1] Jeftenić, B., et al., Controlled Multi-Motor Drives, *Proceedings*, International Symposium on Power Electronics, Electrical Drives, Automation and Motion-SPEEDAM, Taormina, Italy, 2006, pp. 14-59
- [2] Brandenburg, G., New Mathematical Model For Web Tension and Register Error, *Proceedings*, 3<sup>rd</sup> International IFAC Conference on Instrumentation and Automation in the Paper, Rubber and Plastics, Brussels, Belgium, 1976, Vol. 1, pp. 411-438
- [3] Koc, H., et al., Modeling and Robust Control of Winding Systems for Elastic Webs, *IEEE Transactions on Control Systems Technology*, 10 (2002), 2, pp. 197-208
- [4] Young, G. E., Reid, K. N., Lateral and Longitudinal Dynamic Behavior and Control of Moving Webs, *Journal of Dynamic Systems, Measurement, and Control*, 115 (1993), 2B, pp. 309-317
- [5] Rosato, D. V., Rosato, D. V., *Extrusion*. In: *Plastics Processing Data Handbook*, Springer, New York, USA, 1990
- [6] \*\*\*, Simoreg DC-Master, Microprocessor-Based Converters from 6kW to 2500kW for Variable-Speed DC Drives, Operating Instructions, <https://rb.gy/xqdyo>
- [7] Mitin, F., Krivushov, A., Application of Optimal Control Algorithm for DC Motor, *Proceedings*, 29<sup>th</sup> DAAAM International Symposium on Intelligent Manufacturing and Automation, Vienna, Austria, pp. 0762-0766

- [8] Gu, Z., et al., Fully-digital Tension Control System with PID Algorithm for Winding Ultra-fine Enameled Wires, *Proceedings*, IOP Conference Series: Materials Science and Engineering - IWMSME, Hangzhou, China, 892 (2020), 1, 012064
- [9] Preitl, S., et al., Controller Design Methods for Driving Systems Based on Extensions of Symmetrical Optimum Method with DC and BLDC Motor Applications, *IFAC Proceedings*, 45 (2012), 3, pp. 264-269
- [10] Bettendorf, R., Winder Software Testing With Real-time Dynamic Simulation, *IEEE Transactions on Industrial Electronics*, 52 (2005), 2, pp. 489-498
- [11] Shin, D., et al., Observer Based Non-linear Tension Control for Multi Motor Wire Winding System, *Proceedings*, 12<sup>th</sup> International Conference on Automation and Systems - ICCAS, Jeju, Korea, 2012, pp. 1333-1336
- [12] Nikolić, S. S., et al., Torque Regulation of the Output Pulling Device of the Cable Line for Insulation, *Proceedings*, 20<sup>th</sup> International Conference on Thermal Science and Engineering of Serbia – SIMTERM, Niš, Serbia, 2022, pp. 558-572
- [13] Emhemed, A. A. A., Mamat, R. B., Modelling and Simulation for Industrial DC Motor Using Intelligent Control, *Procedia Engineering*, 41 (2012), Dec., pp. 420-425
- [14] Milovanović, M., et al., Improvement of DC Motor Velocity Estimation Using a Feedforward Neural Network, *Acta Polytechnica Hungarica*, 12 (2015), 6, pp. 107-126
- [15] Bencsik, A. L., Appropriate Mathematical Model of DC Servo Motors Applied in SCARA Robots, *Acta Polytechnica Hungarica*, 1 (2004), 2, pp. 99-111
- [16] \*\*\*, Chapter 12: Three-Phase Controlled Rectifiers, <https://www.coursehero.com/file/10430607/Three-phase-Controlled-Rectifiers/>
- [17] Moran, L., et al., A Three-Phase Active Power Filter Operating With Fixed Switching Frequency for Reactive Power and Current Harmonic Compensation, *IEEE Transactions on Industrial Electronics*, 42 (1995), 4, pp. 402-408
- [18] Lazim, M. T., *Power Electronics and Drives*, Philadelphia University, Amman, Jordan, 2019
- [19] Perdukova, D., et al., *Lyapunov Based Reference Model of Tension Control in a Continuous Strip Processing Line with Multi-Motor Drive*, MDPI, Basel, Switzerland, 2019
- [20] Kocić, I., et al., Single Screw Extruder Temperature Control Using PLC and HMI in Cable Production Process, *Proceedings*, 9<sup>th</sup> International Conference on Electrical, Electronic and Computing Engineering-IcETRAN, Novi Pazar, Serbia, 2022, pp. 137-142
- [21] Landau, I. D., *Adaptive Control*, Springer, Berlin, Germany, 1998
- [22] Uhbehauen H., Rao, G. P., *Identification of Continuous-time Systems*, North-Holland Publishing Co., Amsterdam, The Netherlands, 1987
- [23] Nikolić, S. S., et al., The Winder Dancer Position Control Model Using Different PID Control Structures and Micrologix PLC, *Facta Universitatis Series: Automatic Control and Robotics*, 21 (2022), 2, pp. 77-93
- [24] \*\*\*, <https://t.ly/uHPaW>
- [25] Harnefors, L., et al., Speed Control of Electrical Drives Using Classical Control Methods, *IEEE Transactions on Industry Applications*, 49 (2013), 2, pp. 889-898
- [26] \*\*\*, MicroLogix™ Ethernet Interface, <https://t.ly/iT86w>
- [27] \*\*\*, MicroLogix™ 1200 and MicroLogix 1500 Programmable Controllers, [https://literature.rockwellautomation.com/idc/groups/literature/documents/rm/1762-rm001\\_-en-p.pdf](https://literature.rockwellautomation.com/idc/groups/literature/documents/rm/1762-rm001_-en-p.pdf)
- [28] Raul, P. R., Pagilla, P. R., Design and Implementation of Adaptive PI Control Schemes for Web Tension Control in Roll-to-Roll (R2R) Manufacturing, *ISA Transactions*, 56 (2015), May, pp. 276-287
- [29] Mohamed, M., et al., Robust Sliding-mode Observers for Large-scale Systems With Application to a Multi Machine Power System, *IET Control Theory & Applications*, 11 (2017), 8, pp. 1307-1315
- [30] Xia, J., et al., Two-Degree-of-Freedom Proportional Integral Speed Control of Electrical Drives with Kalman Filter Based Speed Estimation, *IET Electric Power Applications*, 10 (2015), 1, pp. 18-24
- [31] Wang, Z., et al., No-Tension Sensor Closed Loop Control Method with Adaptive PI Parameters for Two-Motor Winding System, *Mathematical Problems in Engineering*, 2018 (2018), 1851845